

# We are IntechOpen, the world's leading publisher of Open Access books Built by scientists, for scientists

6,900

Open access books available

186,000

International authors and editors

200M

Downloads

Our authors are among the

154

Countries delivered to

TOP 1%

most cited scientists

12.2%

Contributors from top 500 universities



WEB OF SCIENCE™

Selection of our books indexed in the Book Citation Index  
in Web of Science™ Core Collection (BKCI)

Interested in publishing with us?  
Contact [book.department@intechopen.com](mailto:book.department@intechopen.com)

Numbers displayed above are based on latest data collected.

For more information visit [www.intechopen.com](http://www.intechopen.com)



# Non-Contact Measurements of the Apparent Density of Green Ceramics with Complex Shape

G.M. Revel, E.P. Tomasini, G. Pandarese and A. Cavuto  
*Università Politecnica delle Marche, Dipartimento di Meccanica, Ancona  
Italia*

## 1. Introduction

The apparent density (or, as often reported in the technical literature, the bulk density) of green ceramic tiles is a fundamental parameter for the quality of final products. In fact, the apparent density determines the entity of the dimensional shrinkage of the ceramic body during firing and is proportional to the mechanical resistance.

In industrial production an irregular shrinkage can be responsible for example for non-planar tiles or residual strengths. Measuring the apparent density allows to control this parameter to limit the production waste and increase the quality of the final product. The apparent density, in the ceramic industries, can be currently measured off-line [Standard UNI EN 1097 - 3, (1999)], and the most used method is generally the hydrostatic weighting in a mercury bath on a small sample [Pei at al, (1999)]. This technique has a limit on the control sample and a continuous mercury use is dangerous for the human health. This, together with ISO 14000 Standard application, poses severe limitations to the use of mercury in Europe, in the United States and other countries. So new methods have been developed to measure the bulk density of ceramic tiles. Some are based on the gas laws utilizing air pressure to determine test specimen volume in a measuring chamber [Dietrich, (1999)], whilst more recent ones are based on X-ray absorption [Amorós at al, (2010)]. The first is a destructive and discrete method, so it is not suitable for on-line application. The second is accurate and non-destructive, but can be expensive and X-ray devices still have some acceptance problems in industry.

In this chapter an innovative method for non-contact measurement of the apparent density of green ceramics is presented, which is also suitable to be used during production. This method, previously developed by the authors, is based on ultrasonic wave propagation within the material. The waves are generated and received by dedicated air-coupled probes. The time of flight is measured in transmission mode on the tile together with the thickness. The thickness can be derived by the ultrasonic signals or, if higher accuracy is required on complex shapes, by a laser triangulation sensor. The velocity of the ultrasound wave can be calculated by these measurements and it is proportional to the apparent density. The conversion factor between velocity and apparent density is evaluated by a calibration procedure with a reference method of known uncertainty (e.g. mercury bath).

The chapter not only summarizes the research steps performed in this field in the last 10 years for measurements both at the laboratory and industrial level, but also presents a new challenging application to pieces with complex shapes.

## 2. Bulk density and ultrasonic propagation

The ultrasound propagation is the physical phenomenon on which the theory for measurement of the apparent density in green ceramics is founded. A probe generates a ultrasound wave that propagates in the medium with a characteristic velocity so the time of flight, given a certain length of the propagation path, can be measured.

In a solid material longitudinal and transversal waves can be propagated. In an isotropic material, the relationships between longitudinal (oscillation along the propagation direction) waves velocity  $v$  and transversal (oscillation orthogonal to the propagation direction) waves velocity  $v_t$  with the elasticity properties of the material are given by [Krautkramer et al, (1983)]:

$$v = \sqrt{\frac{E}{\rho} \cdot \frac{(1 - \mu)}{(1 + \mu) \cdot (1 - 2\mu)}} \quad (1)$$

$$v_t = \sqrt{\frac{E}{\rho} \cdot \frac{1}{2(1 + \mu)}} = \sqrt{\frac{G}{\rho}} \quad (2)$$

where  $E$  is the Young's modulus,  $G$  is the elasticity tangential modulus,  $\mu$  is the Poisson coefficient and  $\rho$  is the bulk density of the material. For a porous body, like a green tile (isotropic in first approximation, as obtained by powder compaction), there are many theoretical models linking the elastic properties with porosity and consequently with the apparent density [Wachtman, (1996)]. Commonly for ceramic bodies, the empiric Spriggs model is used [Spriggs, (1961)], which states that Young's and elasticity tangential modulus exponentially decrease with porosity  $p$ . Porosity can be defined as:

$$p = \frac{\rho_s - \rho}{\rho_s} = \frac{V_a - V_s}{V_a} \quad (3)$$

where  $V_a$  is the apparent (bulk) volume of the body gross open and closed pores, considered as the total volume in the macroscopic external surface of the body, i.e. in its envelope and  $V_s$  is the effective volume of the body net of the closed and open pores;  $\rho_s$  is the average actual density. So the Spriggs model can be written as:

$$E = E_0 e^{-bp} \quad (4)$$

$$G = G_0 e^{-bp} \quad (5)$$

where  $E_0$  and  $G_0$  are the values at null porosity ( $p=0$ ,  $\rho=\rho_s$ ), and  $b$  is a parameter to be experimentally determined, which can differ by some percentage between equations (4) and (5), but it is normally  $b= 4,0 - 4,5$  when  $p= 0 - 40\%$ .

In this approach only the longitudinal waves velocity is considered, because the  $v_t$  is not easily measurable in the industrial application. This is supported by the assumption that the Poisson coefficient is invariant with the apparent density [Revel, (2007)]. The longitudinal waves velocity, like those propagated by a non contact ultrasound probe, are measured

orthogonally to the sample surface and the relationship linking the velocity  $v$  and the apparent density  $\rho$  is obtained by (Eq. 1), (Eq. 3) and (Eq. 4):

$$v = \sqrt{\frac{E_0 e^{-b\left(1-\frac{\rho}{\rho_s}\right)}}{\rho} \cdot \frac{(1-\mu)}{(1+\mu)(1-2\mu)}} \quad (6)$$

In Fig. 1 (a) the function of (Eq. 6) is plotted for typical values (e.g. [Wachtman, (1996)]) for ceramic green tiles ( $E_0 = 6$  GPa,  $b = 4$ ,  $\mu = 0,2$ ,  $\rho_s = 2,600$  g/cm<sup>3</sup>) obtained by traditional mix of raw materials (clays, feldspars, etc.) and with a fixed constant humidity content.

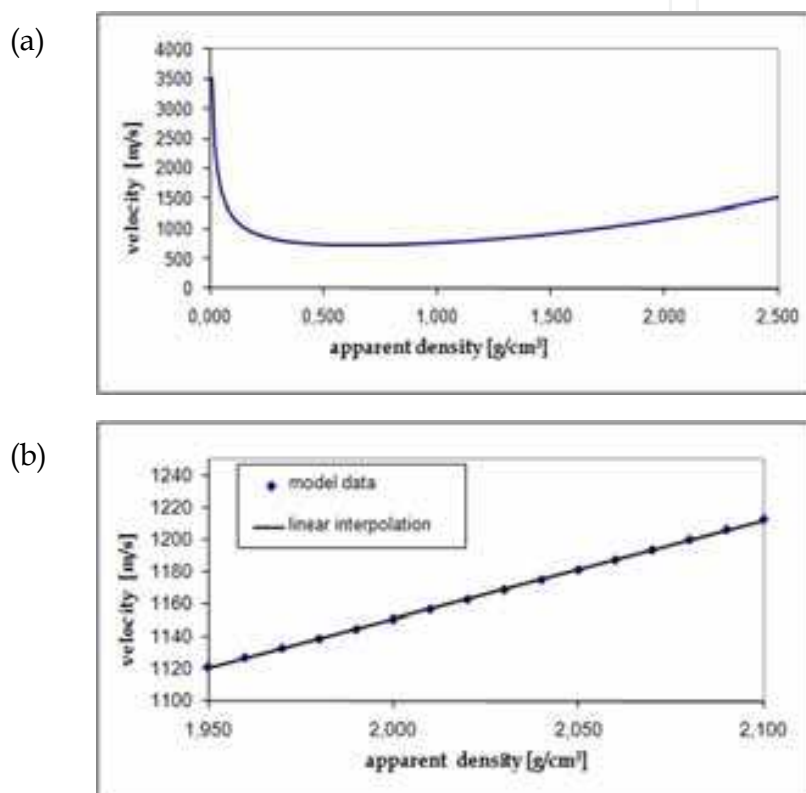


Fig. 1. (a) Plot of the longitudinal waves velocity  $v$  in function of the apparent density ( $E_0 = 6$  GPa,  $b = 4$ ,  $\mu = 0,2$ ,  $\rho_s = 2,600$  g/cm<sup>3</sup>); (b) Zoom of the diagram in a typical range of industrial interest with relative interpolating straight line

The graphic shows that, increasing the apparent density up to porosity values lower than 60 % (i.e. about  $\rho > 1,000$  g/cm<sup>3</sup>), the longitudinal waves velocity tends to increase with an almost linear trend. If a typical range of apparent density of industrial interest for green tiles is considered (Fig. 1 (b)), with a good approximation the model can be considered as linear. In fact the discrepancies between the model's data and their linear interpolation is always lower than 2 m/s (i.e. lower than 0,2 %).

In [Revel, (2007)] the results of a parametric analysis of (Eq. 6) with the variation of  $E_0$ ,  $b$  and  $\mu$  was presented. This analysis clearly showed that the uncertainty on the model parameters can generate significant uncertainty on the results of the correlation between velocity and apparent density. On the contrary the discrepancies caused by the linearization seem to be always very low.

Ultrasound measurements are usually performed with contact probes using film of gel, oil or water as coupling media. This set-up is capable of guaranteeing high signal-to-noise ratio, thanks to the reduced attenuation at the interfaces.

In the case of non contact inspection (air-coupled probes), the propagation path is more complex and the attenuation significantly higher. The energy of the signal that passes through the material in this case is very limited, due to the high difference between the acoustic impedance of the air and of the solid material. In fact, if an ultrasonic wave is propagating from a medium with acoustic impedance  $Z_1$  to another medium with acoustic impedance  $Z_2$ , the reflected signal energy will be proportional to the difference between  $Z_1$  and  $Z_2$ . This is quantified by the coefficients of reflection  $R$  and transmission  $T$  of the sound pressure, defined as:

$$R = \frac{P_r}{P_i} = \left( \frac{Z_2 - Z_1}{Z_2 + Z_1} \right) \quad (7)$$

$$T = \frac{P_t}{P_i} = \left( \frac{2Z_2}{Z_2 + Z_1} \right) \quad (8)$$

where  $P_t$ ,  $P_r$  and  $P_i$  are sound pressures of the reflected, transmitted and incident waves respectively (Fig. 2).

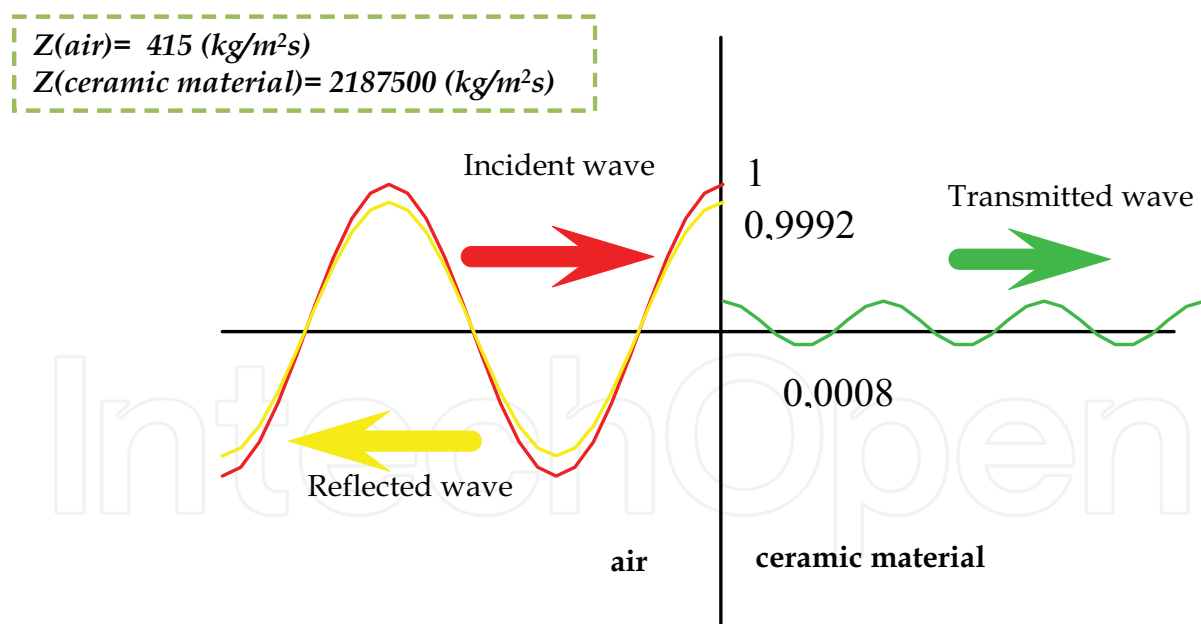


Fig. 2. Scheme of Transmission and Reflection energy: air-ceramic material

In terms of energy, these coefficients become:

$$\bar{R} = \left( \frac{Z_2 - Z_1}{Z_2 + Z_1} \right)^2 \quad (9)$$

$$\bar{T} = \frac{4Z_2Z_1}{(Z_2 + Z_1)^2} \quad (10)$$

As depicted in Fig. 2, if we consider the energy transmitted at a single interface between air and ceramic, this is in the order of about 0,1 %. If multiple reflections are used for time of flight measurement, the wave goes through the interfaces several times, thus creating a dramatic signal attenuation of several order of magnitudes.

Therefore air-coupled ultrasonic techniques require proper signal conditioning (filtering, averaging, signal enhancement, etc.) and measurement set-up to reach an acceptable signal-to-noise ratio (> 20 dB).

On the other hand, this technique offers several advantages:

- possibility of measurement on moving objects or with moving probes;
- easy set-up of a scanning system;
- no contamination of the samples with coupling medium;
- the total production can be inspected with reduced testing time.

### 3. The measurement method - laboratory tests

According to velocity theory the propagation velocity is proportional to the apparent density  $\rho$ . Once the speed is measured, (Eq. 6) could allow to determine  $\rho$ , nevertheless it would be also necessary to know  $E_0$ ,  $b$ ,  $\mu$  and  $\rho_s$ . Considering that these parameters change by tile typology (body, raw materials, etc.), that their measure is very complex and uncertain and that this uncertainty can reduce the accuracy in the apparent density determination, it is not here suggested to use (Eq. 6) to measure  $\rho$ , whilst a more practical approach is proposed.

In the proposed measurement method the time of flight of ultrasound waves is firstly measured with non contact probes in transmission configuration through the tile. The scheme of this measurement method is showed in Fig. 3.

The times of flight are measured with cross-correlation algorithms between the excitation signal of the transmission probe and the received signal.

As shown in Fig. 3 (b),  $t_c$  is the time of flight of the wave from probe to probe through the tile, while  $t_m$  is the propagation time inside the material. A typical cross-correlation signal measured on a green tile is showed in Fig. 3 (c),  $t_c$  is represented by the first peak, while the difference in the time axis between the first and second peak represents  $2t_m$ .

From the time of flight measured in air  $t_a$ , if the distance  $D$  between probes is known, the propagation velocity can be achieved.

In this first approach the distance among the probes membranes  $D$  (= 100 mm in this case) has to be measured using a calliper. It follows that the ultrasound measurement method consists in two steps: (a) measure of the time of flight  $t_a$  of the ultrasound wave in air in the environmental condition of use; (b) measure of the time of flight of the ultrasound wave through the tile body  $t_c$  (where  $t_c < t_a$ ) where, through the measurement of the arrival time of the second echo, it is possible to know also the time of propagation  $t_m$ . These steps are repeated every time a tile passes through the probes during the production.

From the measure in air the propagation velocity of sound in air in the application environmental condition can be derived:

$$v_a = \frac{D}{t_a} \quad (11)$$

It is necessary to often repeat this measure because, as well known, the sound velocity  $v_a$  changes in environmental condition mainly in function of temperature and humidity. For example with a temperature of 20 °C and with relative humidity of 50 % there is a speed of 344 m/s.

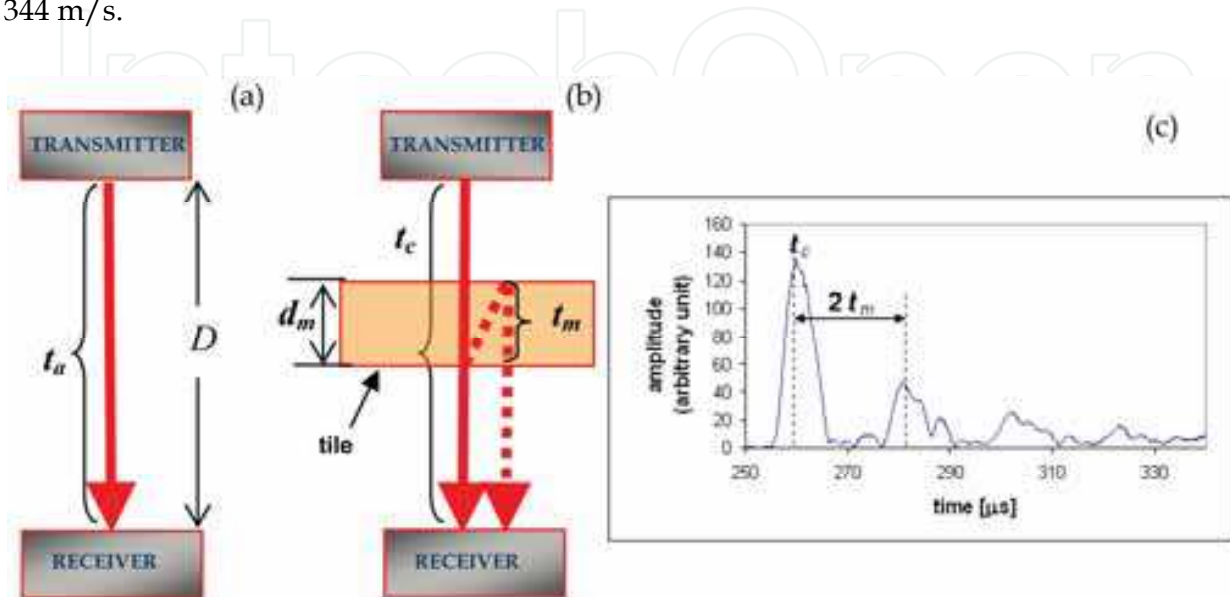


Fig. 3. Scheme of the measurement method: (a) Measurement in air; (b) Measurement on the tile; (c) Example of cross-correlation signal measured on a tile (amplitude in arbitrary unit)

In literature there are many formulas for the sound velocity estimation, for example one can be approximated from [Cramer, (1993)]:

$$v_a(T, \theta) = (331,5 + 0,59 \times T[^\circ\text{C}]) \left( 1 + 0,004 \frac{\theta[\%]}{100} \right) \quad (12)$$

where  $T$  is the air temperature and  $\theta$  the relative humidity.

Nevertheless in order to avoid the measurement of temperature and humidity, it is better to compensate this effect by directly measuring  $v_a$ , especially in the production line where it is not possible to take under control the environmental conditions.

By the measurement of  $t_c$  and  $t_m$  the average thickness of the tile in the area of the ultrasonic beam (about 1 cm<sup>2</sup>) can be obtained

$$d_m = D - v_a(t_c - t_m) \quad (13)$$

and in the end the propagation velocity of longitudinal waves as:

$$v = \frac{d_m}{t_m} \quad (14)$$

Considering that in the range of interest Eq. 6 can be considered as linear with an error lower than 0,2 %, it is proposed to determine a linear experimental correlation between

velocity and apparent density. This relationship can be obtained by an experimental calibration procedure to be carried out with a reference method of known uncertainty, such as the one based on mercury.

The Fig. 4 provides an example of correlation diagram, which can be later used to determine the apparent density of unknown samples, once measured the propagation velocity.

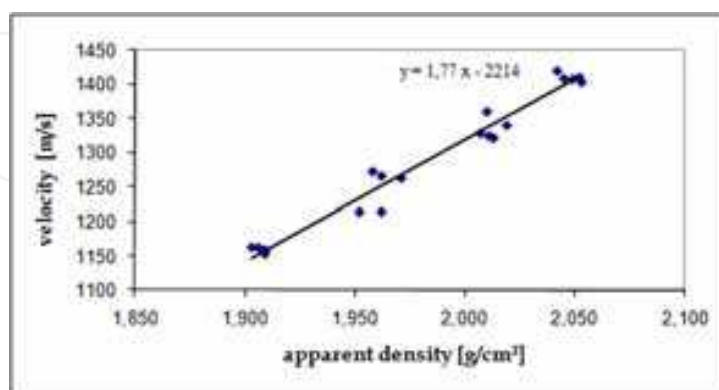


Fig. 4. Correlation diagram (with relative straight fitting line) between longitudinal wave velocity and apparent density measured on green ceramic tiles

In reality also the humidity content has an influence on the propagation velocity, but this effect is considered negligible when measurements are performed on dried tiles or on tiles with constant humidity level. A preliminary attempt to deal with the humidity influence on such ultrasonic measurements has been presented in [Cantavella et al, (2006)]. The problem of moisture influence in on-line measurements has been tackled by the authors in [Revel et al, (2009)] and [Rivola et al, (2007)] and will be discussed in the next chapter.

The experimental apparatus used in the first investigations was based on piezoelectric probes [Bhardwaj, (2002)] with a membrane diameter of 12,5 mm working at around 1 MHz. Air coupled piezoelectric probes have usually a dedicated layer of low impedance material (porous plastic, pressed fibres, polymers, etc. depending on the specific patent) placed between the piezoelectric crystal and the air, in order to reduce the impedance difference between emitting element and air.

Green ceramic tiles having flat faces on both sides, produced in laboratory, have to be used as calibration samples. The planarity of the sides allows to have a higher SNR because the grid in the rear side of the tile represents a modifying input for the ultrasound measurement, caused by the effects of diffraction and thickness variations. In addition, the samples are dried in order to avoid any effect due to moisture. For the calibration of Fig. 4, 20 samples of known density (5 samples for 4 different pressing levels) were used. The propagation velocity was measured in a point of each sample with 200 averages on the signal. It is worth to underline that the determined parameters are valid only for ceramic green tiles with body and raw materials used for the calibration samples. In industrial field, it is necessary to repeat the calibration with every change of body. Examples of correlation diagrams achieved for 3 different kinds of clay and body are reported in Fig. 5, showing the possibility of generalizing the method.

Therefore measurement of the apparent density with the proposed method consists of 3 main steps (once fixed and measured the distance  $D$  between the probes):

**Step 1.** times of flight measurement.

**Step 2.** estimation of the longitudinal waves velocity through.

**Step 3.** experimental correlation between velocity and apparent density through calibration.

In each step there are uncertainty components which could be generated and propagated up to the final results. In order to optimize the measurement process, it is necessary to determine the weight of each uncertainty source on the final results. This has been addressed in detail in [Revel, (2007)] where it is shown that the method guarantees an uncertainty below  $\pm 0,009 \text{ g/cm}^3$ .

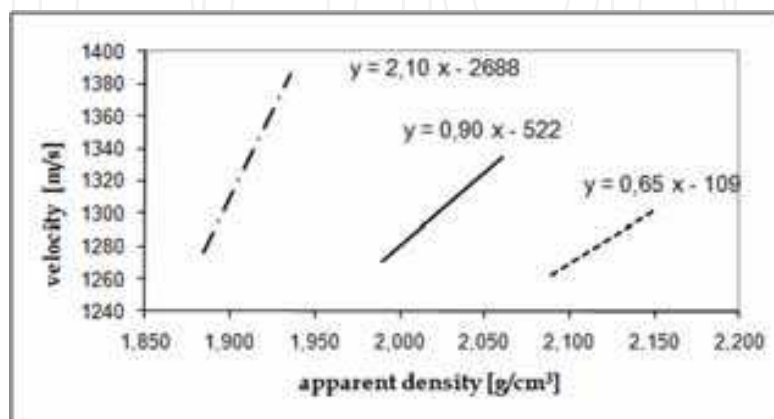


Fig. 5. Examples of correlation diagrams achieved on green tiles with different raw materials and body

#### 4. Industrial application

After some years of research in the EU funded project SENSOCER techniques based on non-contact ultrasonic probes have been developed to properly measure the bulk density of ceramic tiles directly on the line after pressing. These systems are based on air-coupled electro-capacitive transducers and laser triangulation sensors for the detection of the thickness. They have recently demonstrated enough accuracy for industrial applications (repeatability below  $0,01 \text{ g/cm}^3$ ) [Revel at al, (2009)] and are being now exploited in an industrialisation phase, after application of an international patent [Rivola at al, (2007)]. The measurement apparatus is conceived to monitor both the average production value and the spatial distribution of the bulk density and takes into account the effect of moisture content on the measurement accuracy.

The on-line system is a development of the basic one described in the previous Par. 3 for laboratory tests [Revel, (2007)], upgraded for further improvement of accuracy and flexibility. It is constituted by electro-capacitive transducers and a couple of laser triangulation sensors. The electro-capacitive transducers, specifically developed for the application, are driven by a Metalscan ultrasonic board and have an active area diameter of 20 mm and a working frequency of 190 kHz. They have been chosen for this application because of their high sensitivity, in particular in the low frequency range. They are set in a through-transmission configuration for measuring the time of flight of the ultrasonic signal through the tile, while the laser triangulation systems, M7L/10-B24 produced by MEL, measure the tile thickness. Thanks to these devices, it is possible to evaluate the ultrasound velocity  $v$  in the green ceramic tiles, using equation 14.

The main difference with respect to the method in Par. 3 is that the thickness is independently measured (by the laser probes) and it is not derived using the same ultrasonic signals. From one side, this makes the system more expensive and complicated, but on the other hand the accuracy is improved. Therefore, if the basic system was already able to guarantee an uncertainty in the order of  $\pm 0,009-0,01$  g/cm<sup>3</sup>, here the performances are better (uncertainty in the order of  $\pm 0,006-0,007$  g/cm<sup>3</sup>, having an accuracy on the measurement of the thickness of  $\pm 0,02$  mm). In addition, since the thickness has not to be measured by ultrasounds, a lower frequency can be used (190 kHz), allowing lower attenuation in air and thus higher *signal-to-noise* ratio (30 – 34 dB in this work with 200 averages for each acquisition). This solution showed to be the best one also for the application on complex shapes as will be reported in next Par. 5.

In the production line there is very few time for the measurement and for a good calibration it is important to measure the real produced tiles. So the linear correlation between apparent density and velocity, at the production moisture level, has been estimated using samples taken directly from the line at 3 different density levels (achieved with 3 different pressure levels varying about 70 bar above and below the normal press operating conditions, of 444 bar).

Concerning the effect of the moisture on the ultrasound measurements, it is known that moisture decreases the propagation velocity [Cantavella at al, (2006)], so also the influence of this parameter was evaluated to guarantee the required uncertainty (max  $\pm 0,009-0,01$  g/cm<sup>3</sup>).

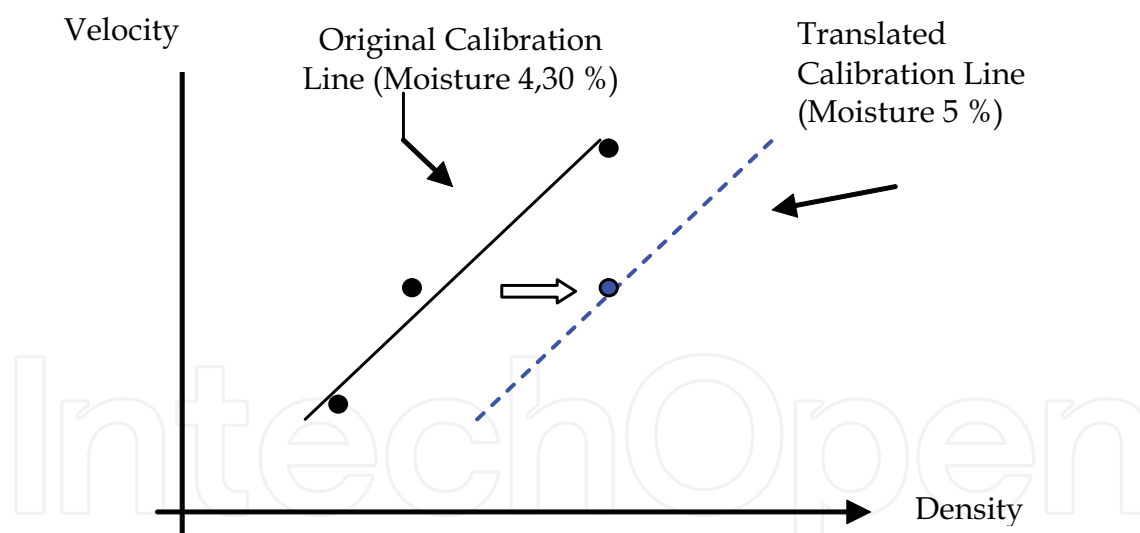


Fig. 6. Adjustment of the calibration line to different moisture values

An extensive sensitivity analysis performed during the SENSOCER project demonstrated that, on average, humidity variations higher than 0,3 % can cause a deviation in apparent density measurements in the order of 0,005 g/cm<sup>3</sup>. To deal with this problem, two methods have been implemented and tested. In the first one, the results of continuous humidity measurements using an IR probe serve as a correction factor when evaluating the density readings. Long on-line observations showed, however, that in many cases the variations are lower than 0,3 % for many hours. Thus a second method, simpler and cheaper but less accurate, has been introduced. Here, the moisture content is manually measured by an



the average density of the products; b) information on the average spatial density distribution.

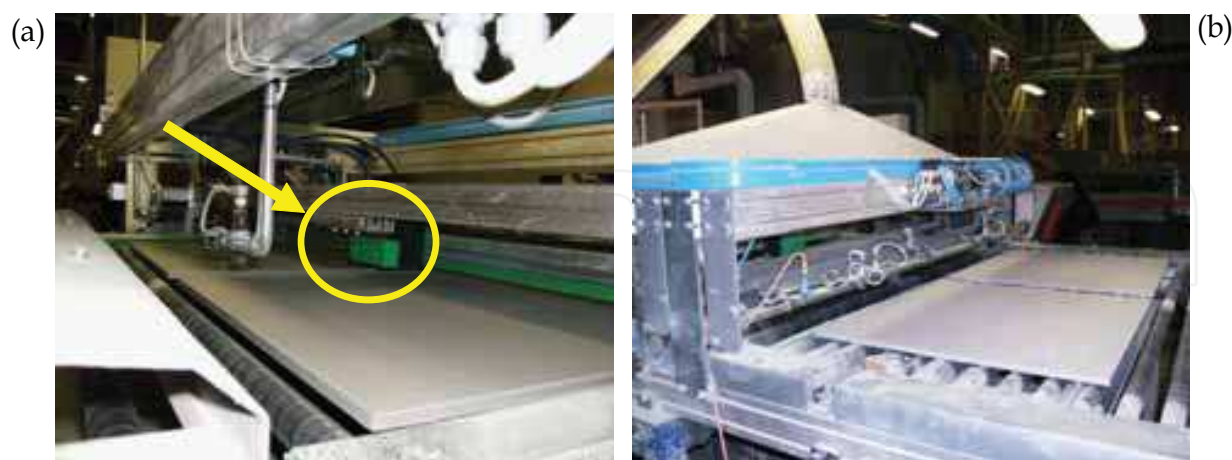


Fig. 8. (a) Head with the sensor holder; (b) Support for on-line positioning

Averaging (both the mean value and spatial distribution) ensures that corrective action on the press is taken only in the event of systematic problems (e.g. wear of a die, non-uniformity in powder loading, significant variations in powder moisture, etc.) and not due to local or instantaneous deviations of the measured values.

The results obtained from measurements on a 60 cm × 60 cm format with a regular rectangular grid on the back are shown. The tile surface is divided into 9 square areas of 20 cm × 20 cm. For the sake of better clarity, the combinations of the areas along the X or Y axis are defined as zones and marked with the number of the first and last included areas (Fig. 7 (b)). For these tests, only 6 areas have been monitored, neglecting the last zone of the tile (zone X), thus reducing the necessary production controller modifications to a minimum.

In order to simulate a production variation, the pressure was increased by 60 bar.

The interval where the pressure has been varied (from tile 24 to tile 40) was detected by the system in its whole duration, with an increase in the average apparent density of about 0,016 g/cm<sup>3</sup>. Some few samples have been taken from the line and measured with the mercury-based method, which revealed a maximum deviation of about 0,005 g/cm<sup>3</sup>. In order to confirm the possibility of predicting variations in the tile dimensions (calibre) after firing, i.e. dimensional shrinkage, each single measured tile was marked and its dimensions after firing were measured.

Fig. 9 (b) illustrates the calibre trend measured along Zone 5-6 for the same tiles, whose apparent density measurements on the Area 5 are plotted in Fig. 9 (a). The trend clearly confirms the behaviour expected from the ultrasonic measurements: the increase in pressure generates higher density and, consequently, larger tile dimensions. In addition, it is possible to note that in both the apparent density and the calibre measurements there is a correlated drift: in fact, their average values at the beginning and at the end of the interval considered seem to increase, probably due to a variation in the moisture content.

The Fig. 9 (a) shows also the relative moving average used to highlight the trends on the single investigated area (with a delay of some samples, due to the algorithm itself). This drift is thus well predicted by the proposed method.

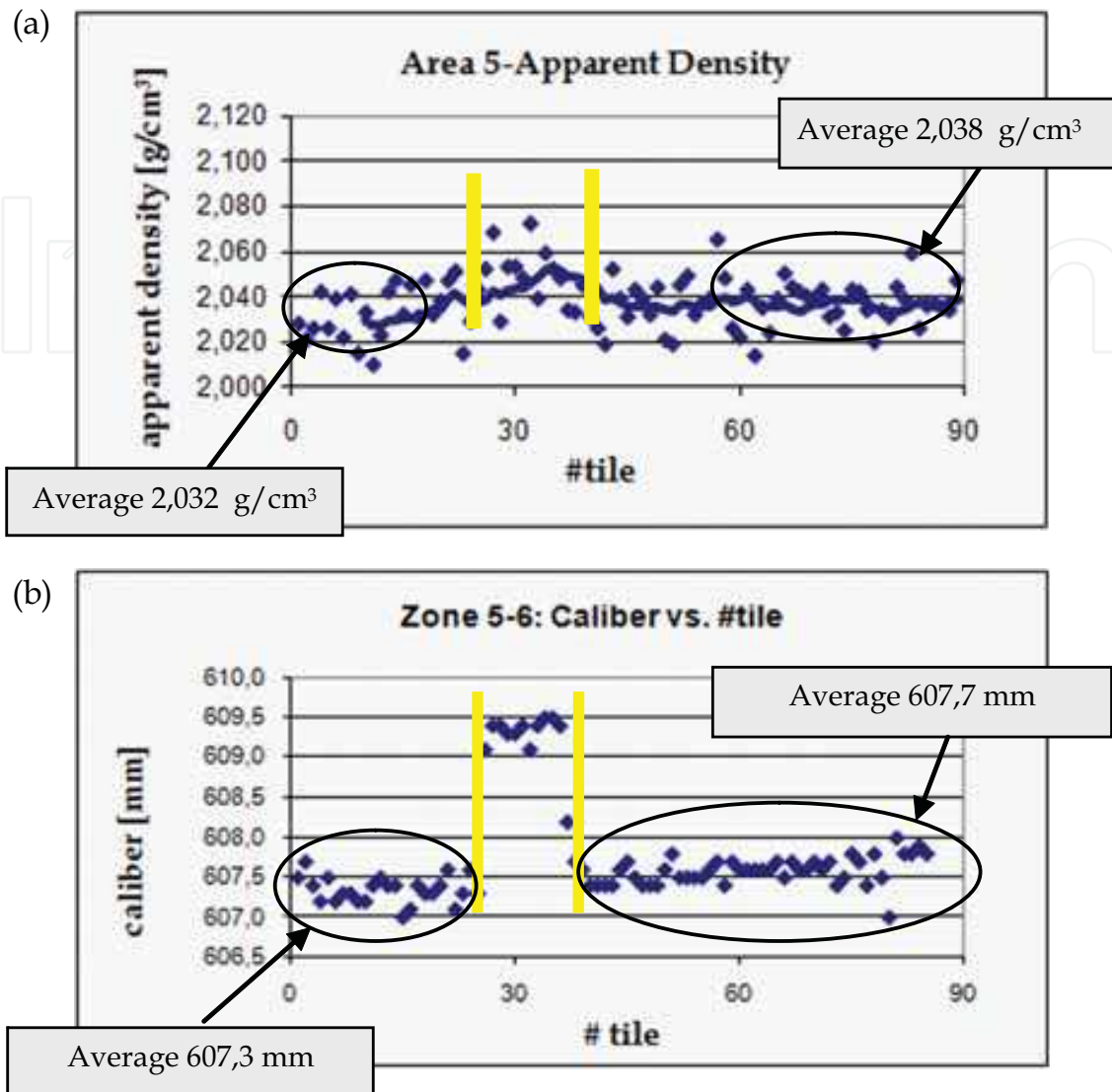


Fig. 9. (a) On-line apparent density measurement for Area 5 in consecutive tiles: the continuous lines represent the interpolation curve obtained with a moving average evaluated on 10 samples; (b) Tile dimension (caliber) trend along Zone 5-6 (measured after firing)

## 5. Advanced application on complex shapes

An additional new goal for the developed non-contact measurement techniques is to inspect also ceramic bodies with complex shape. In tile industry this is becoming of wide interest, due to potential irregular compaction achieved by new production processes.

Here therefore a feasibility study of the method applicability on tiles with high thickness variation and irregular superficial profile (see Fig. 10) is approached. The test has been focused on the central part of the tile, which presents relevant thickness variations higher than a normal tile. The monitoring of the central part is an important achievement, as this is the part with lower strength section: a strong density gradient here is reflected in dimensional and angular problems also in the other 3D parts.

This study was performed in laboratory using the low-frequency electro-capacitive ultrasonic probes (working frequency 190 kHz) interfaced with a dedicated acquisition board, plugged into a PCI slot of a personal computer.

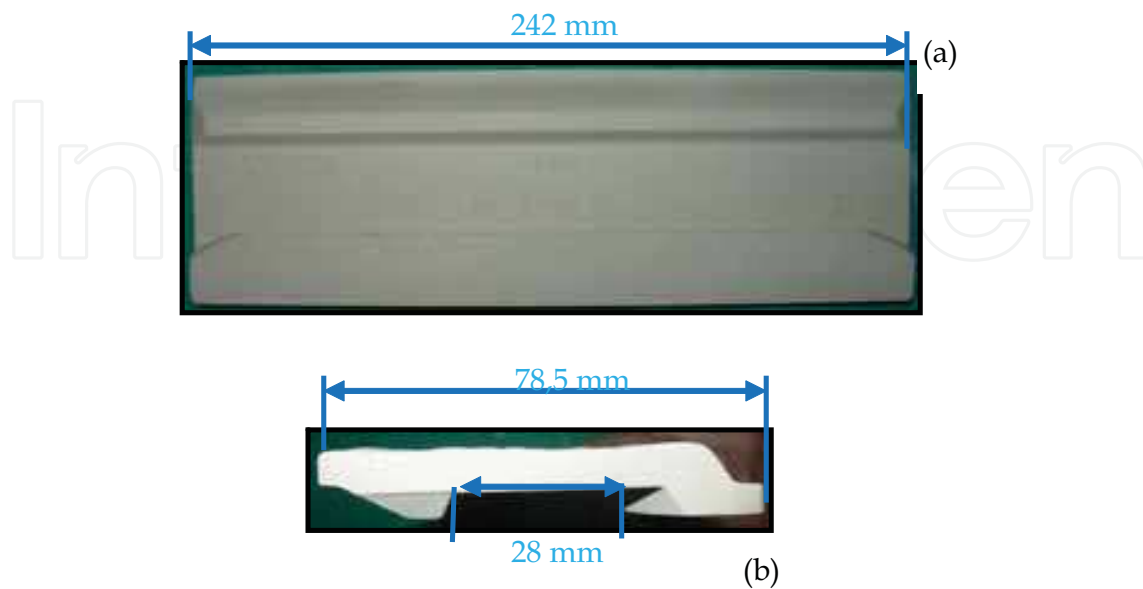


Fig. 10. Tile: (a) Bottom view; (b) Lateral view

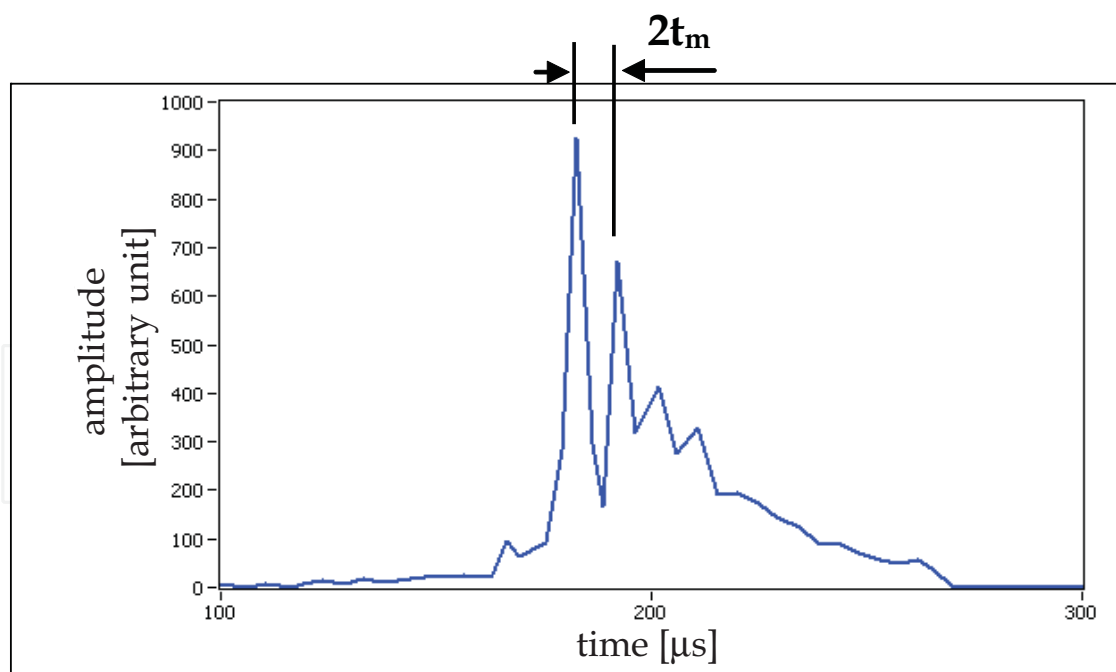


Fig. 11. Waveform of cross-correlation between signal in air and signal through the material

Following the developed procedure, firstly the time of flight  $t_a$  of the ultrasound wave in air in the environmental condition of use is measured by acquisition with no samples between the probes. Then the time of flight in the material  $t_m$  is measured with cross-correlation algorithms between the signal in air without sample and the signal with the sample between

the probes (300 averages for each acquisition). An example of cross-correlation signal is shown in Fig. 11, demonstrating the good quality of the measurements. The thickness was independently measured with two laser triangulation sensors (Laser Mel M5L, resolution 6  $\mu\text{m}$  and laser Keyence LC-2100, resolution 0,5  $\mu\text{m}$ ).

The system was calibrated with four laboratory planar samples at know density (referred to mercury bath measurements performed by the tile manufacturer). The samples had different compaction and were manufactured using same batch composition of the production tiles. For each calibration sample, time of flight and thickness were measured. Fig. 12 shows the achieved calibration line, i.e. the relationship between velocity and bulk density.

After calibration, the system was applied on the real tiles firstly in laboratory conditions and then in simulated on-line tests.

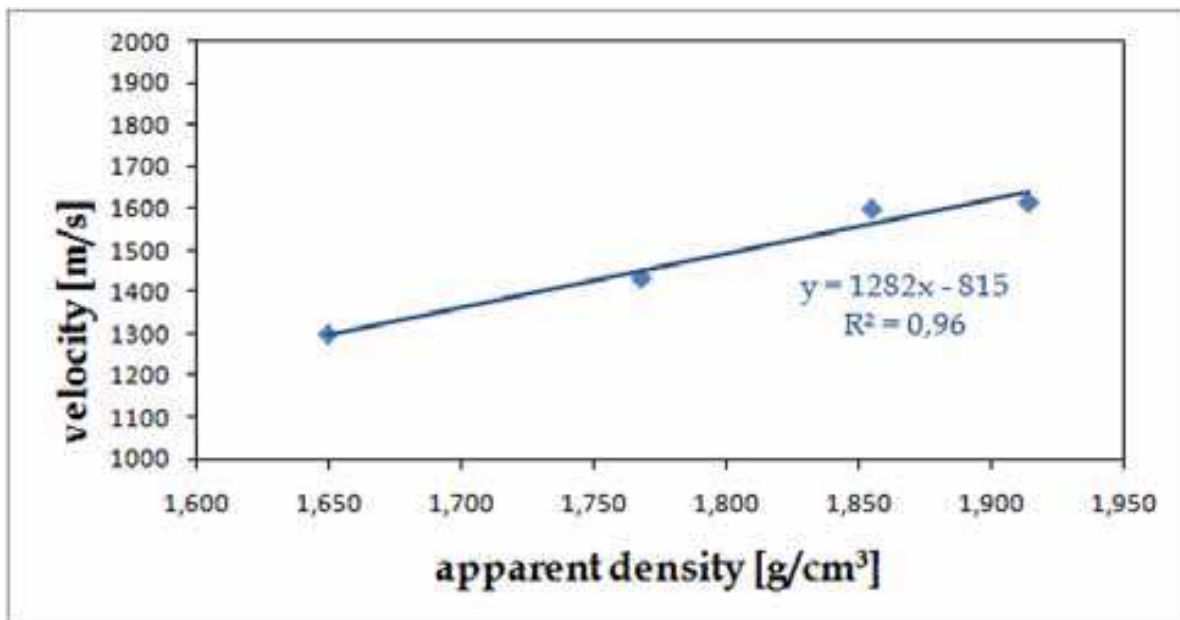


Fig. 12. Calibration line

### 5.1 Test in laboratory conditions

To verify the calibration line and the measurement system on the real tile with complex shape, tests were performed on the central portion of the tile using a manual planar scanning system for transducers. The analyzed portion was divided in 3 zones (Fig. 13 (a)), each having dimensions of 24x32 mm, thus comparable with the diameter of the ultrasonic transducer. In each area the propagation velocity was measured using an average thickness for each of them. The average thickness was evaluated by measuring 5 points taken randomly within each area.

Using the calibration line shown in Fig. 12, once velocity is measured, a density value can be estimated for each zone. In order to have a reference for the achieved values, the 3 areas have been cut and for each of them bulk density was measured with hydrostatic buoyancy method with the samples sealed by wax. This method has a lower accuracy (about  $\pm 0,01$  g/cm<sup>3</sup>) with respect to the mercury bath (about  $\pm 0,002$  g/cm<sup>3</sup>), but it was the only one available in our lab. Comparison results are reported in Table 1: it is shown that the growing

density trend is well detected, even if the thickness variations are relevant, with an average discrepancy of about 0,024 g/cm<sup>3</sup>. This discrepancy is slightly higher than expected, but this can be also due to the lower accuracy of the hydrostatic buoyancy method used as reference.

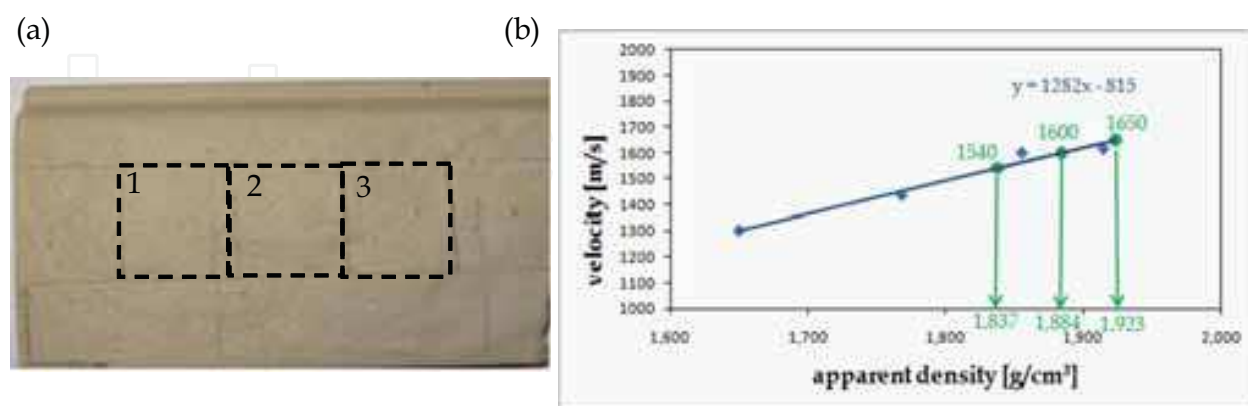


Fig. 13. (a) The 3 investigated areas; (b) Bulk density measured by calibration line (green values)

Zone	Average Thickness (mm)	Velocity (m/s)	Apparent density Ultrasonic method/buoyancy method (g/cm <sup>3</sup> )	$\Delta$ (g/cm <sup>3</sup> )	$\Delta$ (%)
1	8,74	1540	1,837/1,807	0,030	1,7
2	8,52	1600	1,884/1,856	0,028	1,5
3	7,85	1650	1,923/1,908	0,015	0,8

Table 1. Measurement results on the 3 considered zones

### 5.2 Tests in simulated on-line conditions

In order to simulate on-line measurements, an automatic planar scanning system was used to move the ultrasonic and laser triangulation transducers with a 1 mm step while the tile was at rest (Fig. 14). So in this case the probes are moved, but in a real on-line installation it could be possible to use the tile movement to acquire thickness and density profiles.

Whilst the density measurements in Par. 5.1 are related to an area of 24x32 mm, here the density profile is measured along a longitudinal section of the tile using a now approach. Fig. 15 shows the measured thickness profile and morphological reconstruction of the tile.

The tile thickness profile seems to be quite irregular with maximum deviations up to 3 mm. This probably can also lead to expect bulk density and compaction variations along the profile. There construction of the propagation velocity profile was made along the same longitudinal section in the middle of the tile, where the time of flight was measured. The

edges with variable thickness were not considered, as it was assessed that here ultrasound beam propagation is complex and depends on the size of the probes, incidence angle and scattering phenomena.



Fig. 14. The scanning system with ultrasonic and laser triangulation transducers

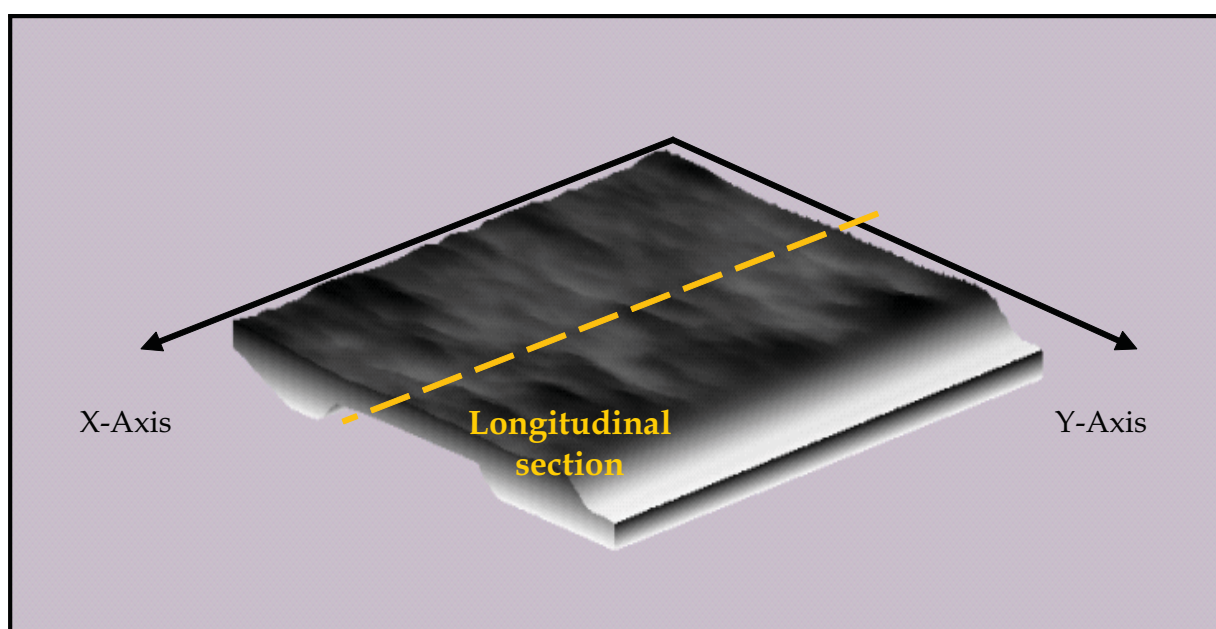
It is worth noting that, whilst thickness measurements by triangulation laser systems are punctual, the times of flight are measured in an area as large as the beam size (about 20 mm). So, even if also the ultrasonic probes are moved by the scanning system at steps of 1 mm, there is the need to define which thickness value has to be associated to the times of flight measured at each different step. It is clear that it has no sense to associate to the measurements performed at one position the single thickness value measured by the laser on the same ultrasonic probe axis position.

As a consequence, it has been decided that, in order to take into account an average thickness within the beam area, a moving average algorithm was adopted: the idea is that, from one position to the next one, the average thickness value is updated discarding the first value (now outside the beam area) and considering the new last value (just entered in the beam area).

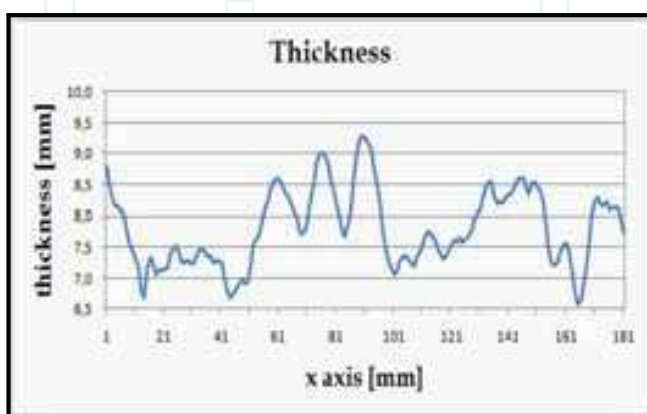
Fig. 16 shows respectively: the raw data of the thickness profile along the longitudinal section indicated in Fig. 15 (a) and the relative moving average; the times of flight along the same section and, finally, the velocity/density along the longitudinal section calculated from the "moving average" thickness. As an example of the adopted procedure the first time of flight value is measured with the ultrasonic probe axis placed in  $x=10$  mm. At this value, the moving average thickness value computed with the first 20 sample (i.e.  $x=20$  mm in Fig. 16 (a)) is associated to estimate velocity and density. The use of the moving average

allows to achieve a sort of continuous bulk density profile (with 1 mm spatial resolution), which can be useful to evaluate undesired trends. It is clear that, from one point to the other, many information are overlapping. So, it could also be useful to estimate average values for larger areas (e.g. 20 mm as the beam size): this can be easily done from the measured data and results are reported in the same graph of Fig. 16 (c). On these values also error bars with amplitude proportional to the uncertainty estimated in previous Paragraphs are reported.

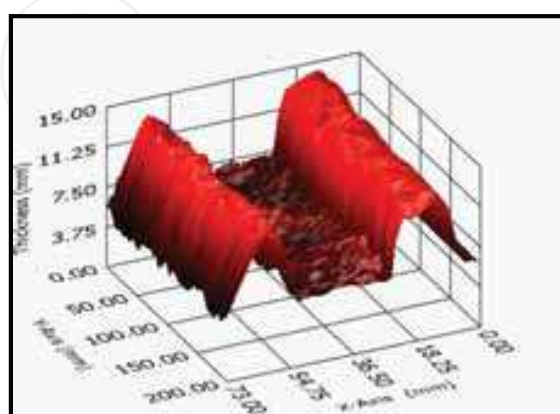
Measured density distribution seems to be coherent with the sample values measured in Par. 5.1. In addition it can be noted that thickness and density profiles tends to have inversely proportional trends, which is coherent with the compaction process, thus demonstrating the feasibility of the proposed measurements.



(a)



(b)



(c)

Fig. 15. (a) Morphological reconstruction of the tile; (b) Thickness profile along the longitudinal section; (c) Tile thickness distribution

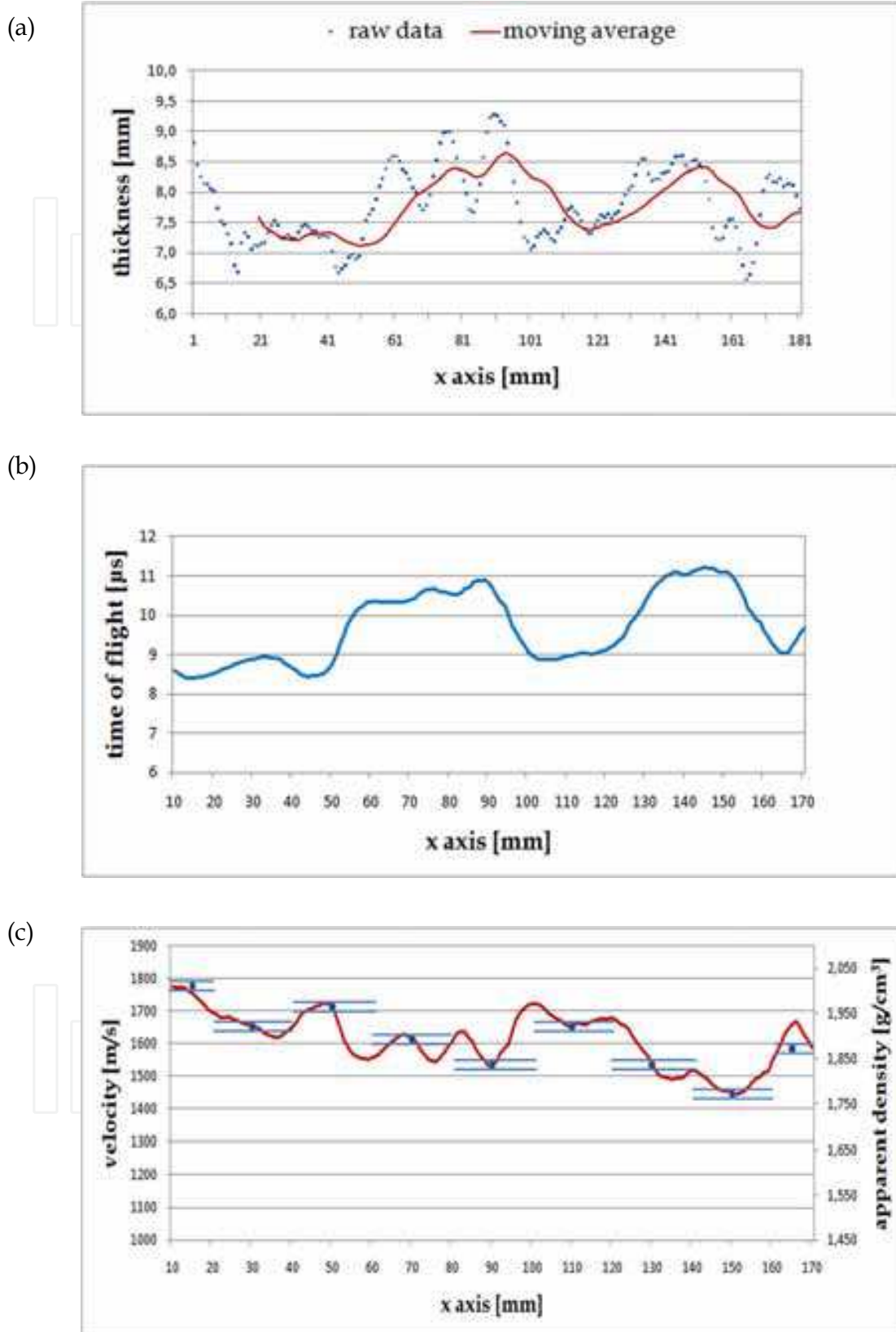


Fig. 16. Diagrams of: (a) Thickness (raw data and moving average); (b) times of flight and (c) velocity/density estimated with “moving average” thickness, with discrete average values computed on 20 mm lengths superimposed

## 6. Conclusion

This Chapter has shown the complete development of the non-contact ultrasonic method for the laboratory and on-line measurement of apparent density on green ceramic tiles. The research was developed in several years and the outcomes have been protected by an international patent. Both the basics of the method and experimental set-ups for laboratory and on-line applications are described, showing that the system is capable of tracking average production values and spatial distribution of apparent density with the industrially required accuracy (max  $\pm 0,01$  g/cm<sup>3</sup>).

An original application on green ceramics with complex shape has been also developed and presented. The results showed the feasibility of measuring on parts with irregular thickness variations up to 3 mm. However the method can be further developed to determine the density values even at the edges of the tile where the profile is curve. The main objective will be to implement dedicated post-processing algorithms to identify and isolate the portions of the measurement signals related to the different paths of the ultrasound wave in the tile.

## 7. Acknowledgments

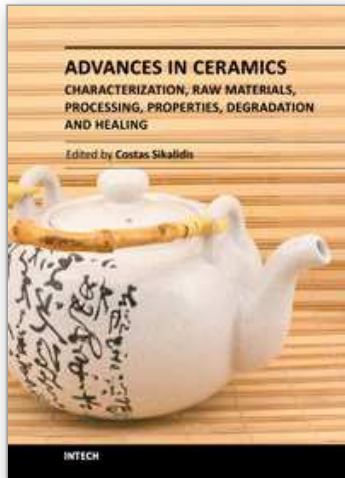
The research has been partly funded by the EU project SENSOCER. The authors would like to thank the company SACMI for the cooperation in the on-line implementation of the prototype. In addition they would like to thank INAX Corporation for the samples with complex shape.

## 8. References

- Amorós, J.L.; Boix, J.; Llorens, D.; Mallol, G.; Fuentes, I. & Feliu, C. (2010). Non-destructive Measurement Of Bulk Density Distribution In Large-Sized Ceramic Tiles. *Journal of the European Ceramic Society*, 30, pp. 2927–2936, Available online at [www.sciencedirect.com](http://www.sciencedirect.com), 12 March 2010
- Bhardwaj, M.C. (2002). High Transduction Piezoelectric Transducers And Introduction Of Non-Contact Analysis, In: *Chapter of Encyclopedia of Smart Materials*, Wiley, J.A. Harvey, (Ed), New York, ISBN 0-471-17780-6
- Cantavella, V.; Llorens, D.; Mezquita, A.; Moltò, C.; Bhardwaj, M. C.; Vilanova, P.; Ferrando, J. & Maldonado-Zagal, S. (2006). Use of ultrasound techniques to measure green tile bulk density and optimise the pressing process, *Proceedings of QUALICER 2006*, Vol. 2, P.BC - 161, ISBN 84-95931-21-4
- Cramer, O. (1993). The variation Of The Specific Heat Ratio And The Speed Of Sound In Air With Temperature, Pressure, Humidity, And CO<sub>2</sub> Concentration, *J. Acoust. Soc. Am.*, 93(5) pp. 2510-2616, ISSN 0001-4966
- Dietrich, E. (1999) *New Measurement Principle for Determining Bulk Density*, EP 0936451.
- Krautkramer, J. & Krautkramer, H. (1983). *Ultrasonic Testing of Materials*, Springer-Verlag, ISBN 3-540-11733-4
- Pei, P.; Minor, D. & Onoda, G. (1999). Laboratory Techniques For Bulk Density Measurement, In: *Advances Process Measurements For The Ceramic Industry*, A. Jillavenkatesa and G. Onoda, (Ed). 293-306, Westerville, OH, ISBN 1574980866.

- Revel, G.M. (2007). Measurement Of The Apparent Volumic Mass Of Green Ceramic Tiles By A Non-Contact Ultrasonic Method, *Experimental Mechanics* 47 pp. 637-648
- Revel, G.M.; Pietroni, P.; Tomasini, E.P.; Pandarese, G. & Cocquio, A. (2009). On-Line Measurement of Green Tiles Apparent Density: Industrial Implementation and Test of an Ultrasonic-Based System, *Tile&Brik International Manual 2009* pp. 42-46. ISSN 0938-9806
- Rivola, P.; Cocquio, A.; Tomasini, E.P.; Revel, G.M.; Pietroni, P. & Pandarese, G. (2007). *A Process For Manufacturing Ceramic Tiles*, WO2007093481AL - 2007
- Spriggs, R.M. (1961). Expression for Effect of Porosity on Elastic Modulus of Polycrystalline Refractory Materials, particularly Aluminium Oxide, *J. Am. Ceram. Soc.*, Vol. 45, 94, , ISSN 0002-7820
- Standard UNI EN 1097 - 3: (1999), *Determinazione della massa volumica in mucchio e dei vuoti intergranulari*, ICS 91.100.15
- Wachtman, J.B. (1996). *Mechanical Properties of Ceramics*, John Wiley & Sons Inc., ISBN: 0-471-13316-7

IntechOpen



**Advances in Ceramics - Characterization, Raw Materials, Processing, Properties, Degradation and Healing**

Edited by Prof. Costas Sikalidis

ISBN 978-953-307-504-4

Hard cover, 370 pages

**Publisher** InTech

**Published online** 01, August, 2011

**Published in print edition** August, 2011

The current book consists of eighteen chapters divided into three sections. Section I includes nine topics in characterization techniques and evaluation of advanced ceramics dealing with newly developed photothermal, ultrasonic and ion sputtering techniques, the neutron irradiation and the properties of ceramics, the existence of a polytypic multi-structured boron carbide, the oxygen isotope exchange between gases and nanoscale oxides and the evaluation of perovskite structures ceramics for sensors and ultrasonic applications. Section II includes six topics in raw materials, processes and mechanical and other properties of conventional and advanced ceramic materials, dealing with the evaluation of local raw materials and various types and forms of wastes for ceramics production, the effect of production parameters on ceramic properties, the evaluation of dental ceramics through application parameters and the reinforcement of ceramics by fibers. Section III, includes three topics in degradation, aging and healing of ceramic materials, dealing with the effect of granite waste addition on artificial and natural degradation bricks, the effect of aging, micro-voids, and self-healing on mechanical properties of glass ceramics and the crack-healing ability of structural ceramics.

**How to reference**

In order to correctly reference this scholarly work, feel free to copy and paste the following:

G.M. Revel, E.P. Tomasini, G. Pandarese and A. Cavuto (2011). Non-Contact Measurements of the Apparent Density of Green Ceramics with Complex Shape, *Advances in Ceramics - Characterization, Raw Materials, Processing, Properties, Degradation and Healing*, Prof. Costas Sikalidis (Ed.), ISBN: 978-953-307-504-4, InTech, Available from: <http://www.intechopen.com/books/advances-in-ceramics-characterization-raw-materials-processing-properties-degradation-and-healing/non-contact-measurements-of-the-apparent-density-of-green-ceramics-with-complex-shape>

**INTECH**  
open science | open minds

**InTech Europe**

University Campus STeP Ri  
Slavka Krautzeka 83/A  
51000 Rijeka, Croatia  
Phone: +385 (51) 770 447  
Fax: +385 (51) 686 166  
[www.intechopen.com](http://www.intechopen.com)

**InTech China**

Unit 405, Office Block, Hotel Equatorial Shanghai  
No.65, Yan An Road (West), Shanghai, 200040, China  
中国上海市延安西路65号上海国际贵都大饭店办公楼405单元  
Phone: +86-21-62489820  
Fax: +86-21-62489821

© 2011 The Author(s). Licensee IntechOpen. This chapter is distributed under the terms of the [Creative Commons Attribution-NonCommercial-ShareAlike-3.0 License](https://creativecommons.org/licenses/by-nc-sa/3.0/), which permits use, distribution and reproduction for non-commercial purposes, provided the original is properly cited and derivative works building on this content are distributed under the same license.

IntechOpen

IntechOpen